Topological and algebraic expressions for the microstructure and septal growth styles of the *Zaphrentis delanouei* species group.

W.A.J. Rutter and M.N. Miliorizos

University of South Wales / Prifysgol De Cymru

Alfred Russel Wallace Building, Glyntaff Campus, Pontypridd, CF37 4BD

A coral in section created from microscope images.

Presented as a poster at Palaeontological Association Progressive Palaeontology 2020

June 2020, Digital Poster

Introduction

The morphology of *Z. delanouei* has been studied previously to determine species phylogeny and ontogeny (Hill, 1939; Hill, 1940; Carruthers, 1908; Carruthers, 1910; Hudson, 1940). Further to the literature, we have carried out an example of a detailed analysis of septal growth using mathematical expressions. The exact methods used are a simple adaptation of a topological technique (homotopic paths within a topological space) and an algebraic expression of micro-fibrous growth lines and their gradients. From path lines drawn out, subsequent trend lines, increments of gradient and sinuosity give a quantitative measure of the **Growth Factor**. Amongst several postulates, it is hypothesized here that the growth rate varies along the coral septa and the growth rate is in direct proportion to all the gradients, expressed here in algebraic form. These are the normalised gradient, T-gradient and sinuosity.

Method 1: Homotopic Paths within Topological Spaces

Utilising methods by Mendelson (1990), the paths between p_0 and p_1 can be described as $F_0 \rightarrow F_1$ with segments between them having different path lengths. The paths follow the arc of concentric circles (akin to the inner and outer envelopes of a septa). Intermediary segments follow curved paths, extending or contracting length of sinuous pathways (akin to growth lines within the micro-fibrous structure of a septa).

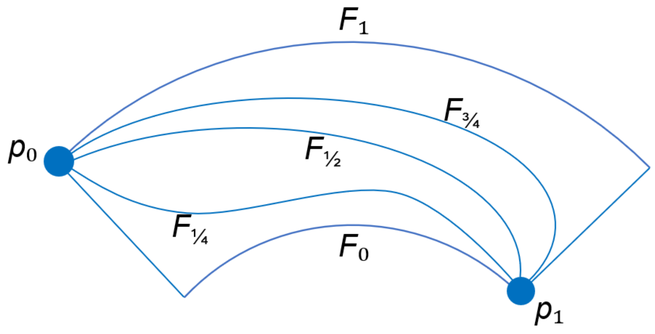

Figure 1: A model of homotopic paths within a topological space (Mendelson, 1990).

Figure 1 shows a representation of homotopic paths within a topological space and increments between F_0 and F_1 in quarter stages.

If F_0 and F_1 are treated figuratively as elastic then over time the paths between them would deform smoothly and continuously. Therefore a path line at time τ = ¼ would fit over a line $F_{¼}$, τ = ½ over $F_{½}$ and τ = ¾ over $F_{¾}$.

Method 2: Algebraic Expression

A uniform and regular grid is drawn over a high resolution image of a septa and the regular horizontal intervals are labelled a – l (see Figure 3). The following measurements are taken from a path line: the change in Horizontal Width along the x-axis (Dx), or an individual Dx segment that is a residual distance from p_0 or p_1; and, the change in Vertical Height along the t-axis (Dt), perpendicular to the x-axis. Increments of gradient of the path line Dt/Dx are calculated for each segment. The mean of these is obtained and compared to the gradient of a direct line from p_0 to p_1. Then the gradient can be normalised.

Measurement of the sinuosity of a path line is taken by tracing the exact line along a distinctive micro-fibrous structure within the septa. Again, the restored length of this line is compared to the direct length between its end points to calculate a percentage sinuosity.

Measurements are taken of the vertical thickness T of the septa along construction lines drawn through the centre of each cell in the uniform grid. This is repeated for the whole septa, along the x-axis and yields a plot of T versus Dx(int). All values are normalised and represented in the graphs (Figures 4 to 7). Linear, polynomial and exponential best fit lines and curves are plotted and gradients calculated using basic differentiation.

The growth factor for a path line in the septa is obtained from the product of the normalised mean gradient of the path line, a normalised T-gradient and its percentage sinuosity. Different values for the growth factor depend upon the path line (inner, middle and outer) and the type of best fit line (see Table 1).

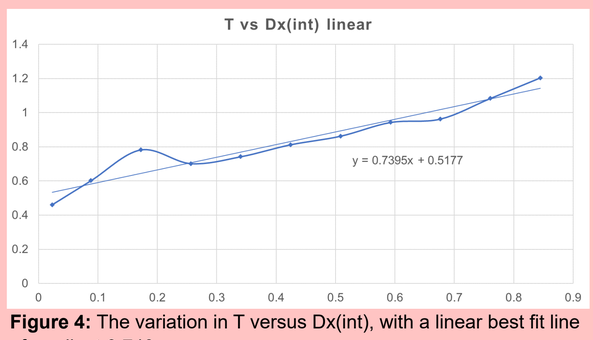

Figure 4: The variation in T versus Dx(int), with a linear best fit line of gradient 0.740.

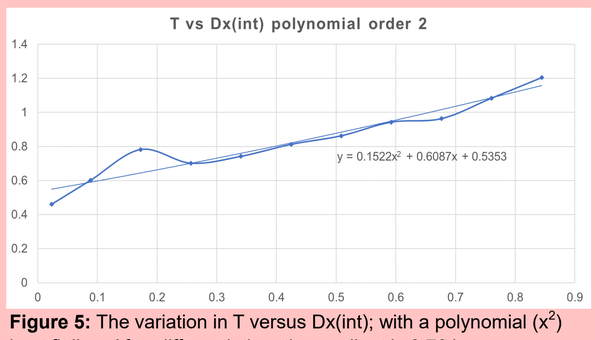

Figure 5: The variation in T versus Dx(int); with a polynomial (x^2) best fit line. After differentiation, the gradient is 0.764.

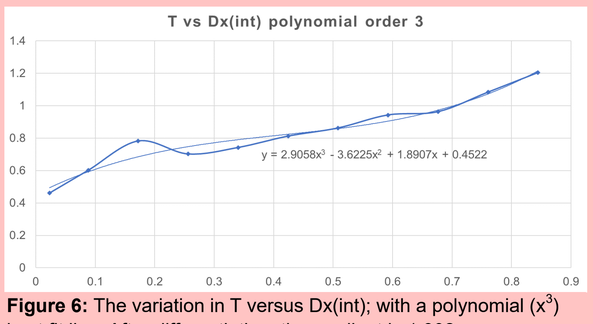

Figure 6: The variation in T versus Dx(int); with a polynomial (x^3) best fit line. After differentiation, the gradient is 1.302.

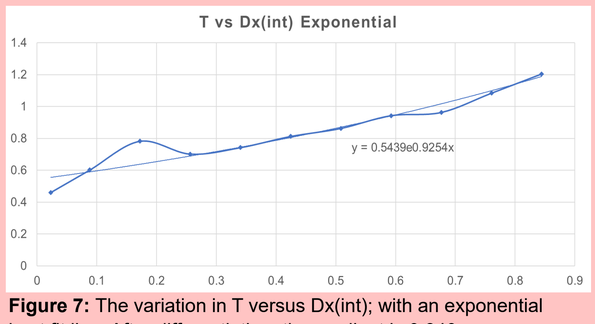

Figure 7: The variation in T versus Dx(int); with an exponential best fit line. After differentiation, the gradient is 0.840.

Table 1: The resultant values for growth factor, obtained from the product of the normalised gradient (Dt/Dx), the gradients of the best fit lines for T/Dx(int) and the percentage sinuosity $[(l_o - l_f)/l_f] \times 100$.

	Linear	Polynomial (x^2)	Polynomial (x^3)	Exponential
1. Outer	0.1027	0.1061	0.1809	0.1167
2. Middle	0.0786	0.0812	0.1384	0.0893
3. Inner	0.0593	0.0612	0.1043	0.0673

Figure 8: A bed of Lower Carboniferous Limestone from the southern tip of Nell's Point, Barry, South Wales, UK. The bioclastic pack-stone contains excellent examples of *Zaphrentis sp.* surrounded by various other marine invertebrate fossils. Direction: west (left), east (right). Scale: 25cm across photograph.

A Major Septa (in detail)

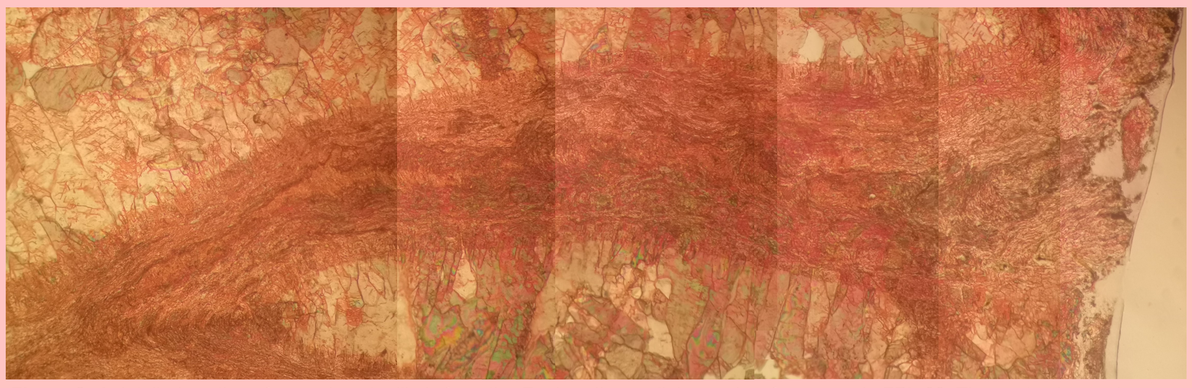

Figure 2: A detailed section of a coral septa, likely from the *Zaphrentis parallela* species, from sample FPL-03. The septa shows clear micro-fibrous growth lines along its length of differing structure that may represent periods of accelerated and diminutive growth.

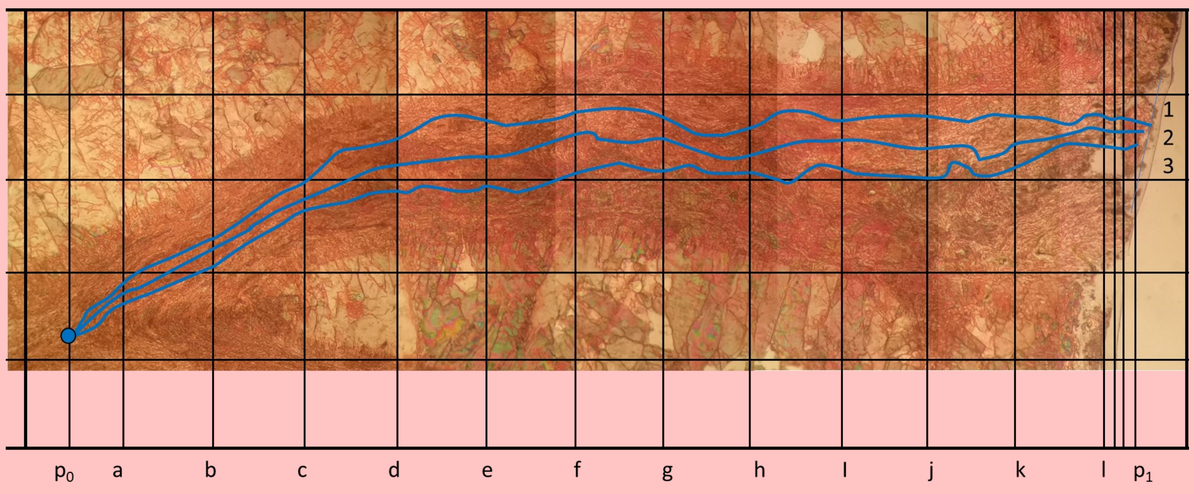

Figure 3: A section of a coral septa with a uniform and regular grid superimposed to facilitate the measurement of the gradients of three path lines along the septa. The path lines are mapped on to growth lines within the micro-fibrous structure.

Discussion

Let us assume(1) the calcareous micro-fibrous septa with its envelope of calcite micro-spar is a ***Topological Space***. Then, by taking ***Homotopic Paths*** along the septa together with an algebraic formulation of its septal structure, a quantitative interpretation of growth style within the septa may be achieved. Now let us assume(2) a figurative ***Topological Elasticity*** for the space between the points p_0(inside) and p_1(outside) both upon the envelope. Then, lines traced [along micro-fibrous structures] within the space between the points p_0 and p_1 are found to follow approximate $F_{¼}$ $F_{½}$ and $F_{¾}$ pathways in a form similar to the path lines shown by the topological model, Figure 1.

From the results, we see consistent weighted gradients for the inner, middle (*syn*. central) and outer path lines (0.927); whilst normalised gradients increase steadily from inner (1.616) middle (1.621) to outer (1.634). Gradients of vertical septal thickness T, plotted against horizontal length along the septa (T-gradient), range between 0.740 and 1.302 depending on the types of best line fit (linear, exponential or polynomial). In addition, the sinuosity of the path lines increases from inner (4.959%) middle (6.557%) to outer (8.502%). Let us assume(3) the septal growth is proportional to the normalised gradient, T-gradient and the sinuosity. Then, a measure of the '***Growth Factor***' may be given by the product of these quantities.

From the results, we see the differences between growth factor for each of the three path lines are similar regardless of the type of best fit line used so that a mean of these gives a growth factor for inner (0.079) middle (0.105) and outer (0.137). Perhaps these differences in growth factor for each path line is somewhat relevant independently and may reflect the style of septal growth from the central structure outwards to the coral wall. That is, the rates of growth along opposing path lines line $F_{¼}$ and $F_{¾}$ may balance with the central path line over $F_{½}$.

The resultant values for growth factor (See Table 1) show a decrease from outer to inner path lines and it is postulated here that the mean growth factor for opposing path lines approaches the growth factor for the central path line. However the added complexity of sinuosity and uneven distribution of septal micro-fibrous structure may point to substantially higher values of growth to one side of the centre and in this example, it is towards the outer path line.

Conclusions

(1) The **rate** of septal growth can be affected by the **direction** or **trajectory** of septal growth (Rutter, 2019). If rate and direction are proportional, then the distribution of calcite in a growing coral, its effective precipitation and spread, permits the construction of an exoskeleton with a morphology that can vary naturally between morphotypes. This natural variability is not just due to the species type of Rugose coral, but is also a response to the immediate environment of existence (Rutter, 2019).

(2) The data presented here, on **Growth Factor,** align well with prior explanations of septal growth within the *Z. delanouei* species group. Hence by inspection, the data offer a tangible basis for a mathematical method to examine and quantify styles of growth in other coral species, fossil and extant.

(3) It is feasible that the micro-fibrous growth inside the coral, in particular along path lines either side of the centre, were restricted or hindered by the style of growth in the coral wall or exoskeleton. Restriction leads to differential stress and asymmetry in micro-fibrous and ultra-microcrystalline growth rate and growth trajectory. Hence, we postulate this asymmetry is either (i) a result of constraint on the position and shape of the soft body and its in-folds or (ii) perhaps a result of advantageous growth in order to maintain a firm structure to protect the coral-zooid during life. Both postulates may lead to the same evolutionary outcome. That is, the overarching control of the exoskeleton, its shape and strength, on the intricate internal structure and growth of a coral: a morphology designed through natural variation for survival amongst a highly abundant benthonic assemblage of invertebrates, beneath the shelf marine waters of the Early Carboniferous.

Key Cited References

Carruthers, R.G. (1908) 'A Revision of some Carboniferous Corals', *Geological Magazine* 5, pp. 20-31; 63-74; 158-171.

Carruthers, R.G. (1910) 'On the Evolution of *Zaphrentis delanouei* in Lower Carboniferous Times', *Quarterly Journal of the Geological Society* 66, pp. 523-538.

Hill, D. (1939) 'A Monograph on the Carboniferous Rugose Corals of Scotland Part II', pp. 79-114, *Palaeontographical Society*, London: Adlard & Son Ltd.

Hill, D. (1940) 'A Monograph on the Carboniferous Rugose Corals of Scotland Part III', pp. 115-204, *Palaeontographical Society*, London: Adlard & Son Ltd.

Hudson, R.G.S. (1940) 'On the Carboniferous Corals: *Zaphrentis carruthersi* sp. Nov. from the Mirk Fell Beds and it's relation to the *Z. delanouei* species-group', *Proceedings of the Yorkshire Geological Society* 24(4) pp. 290-311.

Mendelson, B. (1990) *Introduction to Topology* New York: Dover Publications, Inc.

Rutter, W.A.J. (2019) *Quantitative Modelling of the Zaphrentis delanouei Group, Vale of Glamorgan, UK.* MSc Thesis. University of South Wales.